Quaternary Research 86 (2016) 162–169

Contents lists available at ScienceDirect

Quaternary Research

journal homepage: http://www.journals.elsevier.com/quaternary-research

Timing, cause and consequences of mid-Holocene climate transition in the Arabian Sea

Rajeev Saraswat*, Dinesh Kumar Naik, Rajiv Nigam, Anuruddh Singh Gaur

Geological Oceanography Division, National Institute of Oceanography, Goa, India

ARTICLE INFO

Article history:
Received 13 August 2015
Available online 1 August 2016

Keywords:
Holocene
Climate
Transition
Temperature
Precipitation
Arabian

ABSTRACT

We reconstruct centennial scale quantitative changes in surface seawater temperature (SST), evaporation-precipitation (from Mg/Ca and $\delta^{18}O$ of surface dwelling planktic foraminifera), productivity (from relative abundance of *Globigerina bulloides*), carbon burial (from $\%CaCO_3$ and organic carbon [$\%C_{org}$]) and dissolved oxygen at sediment–water interface, covering the entire Holocene, from a core collected from the eastern Arabian Sea. From the multi-proxy record, we define the timing, consequences and possible causes of the mid-Holocene climate transition (MHCT). A distinct shift in evaporation-precipitation (E-P) is observed at 6.4 ka, accompanied by a net cooling of SST. The shift in SST and E-P is synchronous with a change in surface productivity. A concurrent decrease is also noted in both the planktic foraminiferal abundance and coarse sediment fraction. A shift in carbon burial, as inferred from both the $\%CaCO_3$ and $\%C_{org}$, coincides with a change in surface productivity. A simultaneous decrease in dissolved oxygen at the sediment–water interface, suggests that changes affected both the surface and subsurface water. A similar concomitant change is also observed in other cores from the Arabian Sea as well as terrestrial records, suggesting a widespread regional MHCT. The MHCT coincides with decreasing low-latitude summer insolation, perturbations in total solar intensity and an increase in atmospheric CO_2.

Introduction

Early research suggested that the Holocene was an epoch of relatively stable climate due to limited changes in climatic forcing, which apparently facilitated the rise of civilizations. Recent high-resolution centennial records, however, reveal distinct climatic events in the Indian subcontinent and adjoining seas during the Holocene (Staubwasser et al., 2003a,b; Gupta et al., 2005; Dykoski et al., 2005; Yadav et al., 2011). Such climatic changes during times of limited natural boundary conditions can help in the understanding of Earth's response to increasing anthropogenic influences (Schewe and Levermann, 2012; Cook et al., 2015). The mid-Holocene climatic transition (MHCT) is a very prominent feature of the present interglacial (deMenocal et al., 2000; Weldeab et al., 2005; Roberts et al., 2011; Dixit et al., 2014; Vincenzo and Massimo, 2015). Defining the timing of the MHCT is important as it coincides with distinct changes in human civilizations and has been linked with anthropogenic activities (Ruddiman and Ellis, 2009; Kelly et al., 2013). Previous studies show that the MHCT in the Arabian Sea dates to between 7 and 5 ka (Sarkar et al., 2000; Govil and Naidu, 2010; Singh et al., 2011; Kessarkar et al., 2013; Naik et al., 2014). A centennial-scale multi-proxy record covering the entire Holocene can help better define the timing of the MHCT. A precisely dated MHCT can then be used to help understand the lead–lag relationship between different processes during major climate transitions in the eastern Arabian Sea. Such a record can further help to understand land-ocean interaction and to compare regional climatic events in the context of various global climatic changes. In this paper, we develop a record of mid-Holocene climate changes by using a gravity sediment core (SK237 GC04, hereafter referred as Malabar core) from the continental slope of southeastern Arabian Sea (10°58.65′ N, 74°59.96′ E, water depth 1245 m). The core had centennial scale resolution and covered the last glacial-interglacial transition (Fig. 1). The stable isotopic and trace element analysis of surface dwelling planktic foraminifera from this core was used to define the timing of deglacial warming and precipitation-evaporation changes during the last glacial-interglacial transition (Saraswat et al., 2013). We use multi-proxy analysis on the Holocene section of this core to reconstruct both the surface and sediment–water interface conditions at centennial-scale resolution,

* Corresponding author.
E-mail address: rsaraswat@nio.org (R. Saraswat).

http://dx.doi.org/10.1016/j.yqres.2016.06.001
0033-5894/

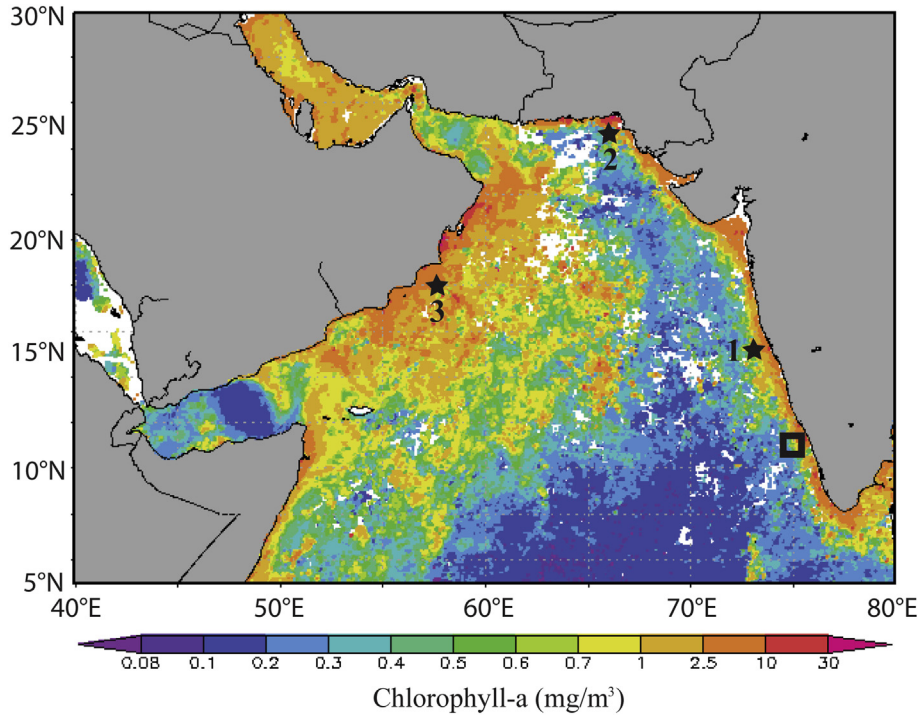

Fig. 1. The core location in the southeastern Arabian Sea is marked by an open black rectangle. Other cores discussed in the text are marked by filled black star (1. SK17, Anand et al., 2008; 2.63KA-41KL, Staubwasser et al., 2003a,b; 3. RC27-23, Altabet et al., 2002). The template is surface primary productivity (chlorophyll-a, mg/m^3) in the Arabian Sea during the southwest monsoon season (June-July-August-September; Acker and Leptoukh, 2007).

throughout the Holocene, to define the timing, possible cause and consequences of the MHCT in the eastern Arabian Sea.

Oceanographic setting

The eastern Arabian Sea is characterized by a seasonal reversal of surface currents in response to winds (Shankar et al., 2002). The equatorward West India Coastal Current brings relatively more saline water to the eastern Arabian Sea prior to and during the southwest monsoon, whereas the poleward winter monsoon current transports low salinity water from the western Bay of Bengal into the eastern Arabian Sea during boreal winter (Prasanna Kumar et al., 2004). Increased productivity in this region is observed during the summer monsoon season (Levy et al., 2007, Fig. 1). The sea surface temperature (SST) in the eastern Arabian Sea increases during the pre-summer monsoon season, leading to the development of a small warm pool that peaks in April. The eastern Arabian Sea warm pool dissipates prior to the onset of summer monsoon precipitation as a result of upwelling (Shenoi et al., 1999). The region is also marked by both seasonal shallow water hypoxic zone (Naqvi et al., 2000) as well as a perennial intermediate water-depth oxygen minimum zone (OMZ) that extends from ~150 to ~1200 m below sea level (Naqvi, 1991; Naqvi et al., 2003).

Materials and methodology

The Holocene section (top 100 cm, subsampled at 1 cm intervals) of the Malabar core was used to reconstruct centennial-scale changes. The section was dated by using five Accelerator Mass Spectrometer ^{14}C ages on mixed planktic foraminifera measured at the Center for Applied Isotope Studies, the University of Georgia, USA (Table 1; Saraswat et al., 2013). Marine09 (Reimer et al., 2009) and Calib6.0 version (Stuiver and Reimer, 1993) were used to calibrate the ^{14}C ages. A reservoir correction (ΔR) of 138 ± 68 yr for the eastern Arabian Sea was applied (Southon et al., 2002). The age model utilizes the calibrated ages as tie-points and assumes a linear sedimentation rate (Fig. 2). A minimum of 300 benthic foraminifera were picked and examined from each sample of the coarse sediment fraction (>63 μm). The relative abundance of angular asymmetrical benthic foraminifera (AABF) was counted following the methods of Nigam et al. (1992, 2007). Planktic foraminifera were picked from the >125 μm sediment fraction. Changes in relative abundance of planktic foraminifera *Globigerina bulloides* (an indicator of high productivity), coarse sediment fraction (CF), organic carbon weight percentage (%C_{org}) and calcium carbonate weight percentage (%$CaCO_3$) were used to reconstruct past monsoon strength and associated changes (Fig. 3). The total %C was measured with a CNS analyzer and inorganic carbon was measured with a coulometer. The precision of total carbon measurements was better than ±0.49%. The precision of total inorganic carbon measurements, based on repeat analysis of laboratory standard after every ten samples, was better than ±0.22%. The %$CaCO_3$ was calculated from the total inorganic carbon. Total %C_{org} was calculated by subtracting total inorganic carbon from the total carbon. The cumulative error associated with %C_{org} estimates was ±0.54%. Seawater paleotemperature was reconstructed from changes in the Mg/Ca ratio of the white variety of planktic foraminifera *Globigerinoides ruber* (Saraswat et al., 2013), which is a very robust method to quantify paleotemperatures (Lea et al., 1999; Saraswat et al., 2005; Weldeab et al., 2005). The error in seawater temperature estimated from Mg/Ca in *G. ruber* is ±1.3 °C. The cumulative error was calculated from the standard deviation of replicate analyses of the samples, when available, combined with the standard deviation of consistency standards during the sample run, as well as the error associated with the calibration equation. The Malabar core data was compared with other records published from the Arabian Sea as well as Indian subcontinent (Fig. 4). Additionally, local evaporation-precipitation changes have been reconstructed by subtracting

https://doi.org/10.1016/j.yqres.2016.06.001 Published online by Cambridge University Press

Table 1
Details of five accelerator mass spectrometer radiocarbon ages obtained on mixed planktic foraminifera measured at the Center for Applied Isotope Studies, the University of Georgia, USA.

Lab#	Sample depth (cm)	^{14}C age (yr BP)	^{14}C age error (±)	Calib. Age-range (1σ) (yr, BP)	Calib. Age-range (2σ) (yr, BP)	Calib. Age (Median probability) (yr, BP)
UGAMS5378	0.5	620	25	0–146	0–246	115
UGAMS5739	25.5	2730	30	2163–2336	2075–2460	2260
UGAMS 23868	35.5	5190	30	5306–5477	5263–5574	5406
UGAMS5740	49.5	6360	30	6580–6760	6484–6846	6670
UGAMS5935	85.5	9930	30	10,556–10,749	10,506–10,940	10,670

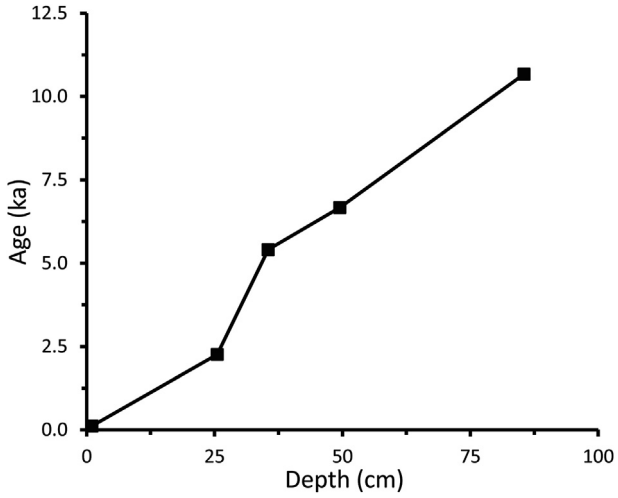

Fig. 2. The age–depth relationship used to establish the chronology of the Holocene section of the core SK237 GC04. The AMS ages were used as tie-points and ages for the intervals between two tie-points, were obtained by linear interpolation. Further details of the age model are discussed in Saraswat et al. (2013).

global ice volume contribution from temperature corrected stable oxygen isotopic ratio ($\delta^{18}O_{sw\text{-}ivc}$) of *G. ruber* (Fig. 5). The error in $\delta^{18}O_{sw\text{-}ivc}$ is assumed to be at least ±0.3‰ because the error associated with $\delta^{18}O_{sw}$ is ±0.3‰ (Saraswat et al., 2012, 2013). The Malabar core data was compared with long-term orbital configuration driven low latitude insolation changes in mid-July at 10°N taken from Laskar et al. (2004), and the total solar irradiance changes from the Steinhilber et al. (2009). The Malabar core record was also compared with the high-resolution lake sediment, speleothem and ice-core records, reconstructed from Asia, to test whether the mid-Holocene transition is confined only to the marine records or is also present in terrestrial Holocene records (Fig. 4), (Enzel et al., 1999; Dykoski et al., 2005; Sinha et al., 2006; Thompson et al., 2012).

Results

Reconstructed Mg/Ca SST varies from 27.3 to 29.5 °C from 2.9 to 11.0 ka. After an initial cooling in SST during the early Holocene, the SST was stable from 9.3 until 6.0 ka (Fig. 3). A net drop in SST is observed during the late Holocene, beginning at 6.0 ka. The most depleted $\delta^{18}O_{sw\text{-}ivc}$ (0.14‰) is evident at 3.6 ka while it is the most enriched (1.19‰) during early Holocene (11.2 ka). A large drop in $\delta^{18}O_{sw\text{-}ivc}$ from the most enriched value of 1.19‰ at 11.2 ka to 0.29‰ at 10.6 ka is evident during the early Holocene immediately after the MIS2/1 transition. The $\delta^{18}O_{sw\text{-}ivc}$ is relatively stable between 9.9 and 6.8 ka. A net decrease with minor fluctuation in $\delta^{18}O_{sw\text{-}ivc}$ is also evident between 6.8 and 6.4 ka. Subsequently a net increase in $\delta^{18}O_{sw\text{-}ivc}$ is evident until 5.3 ka (Fig. 5). Another prominent

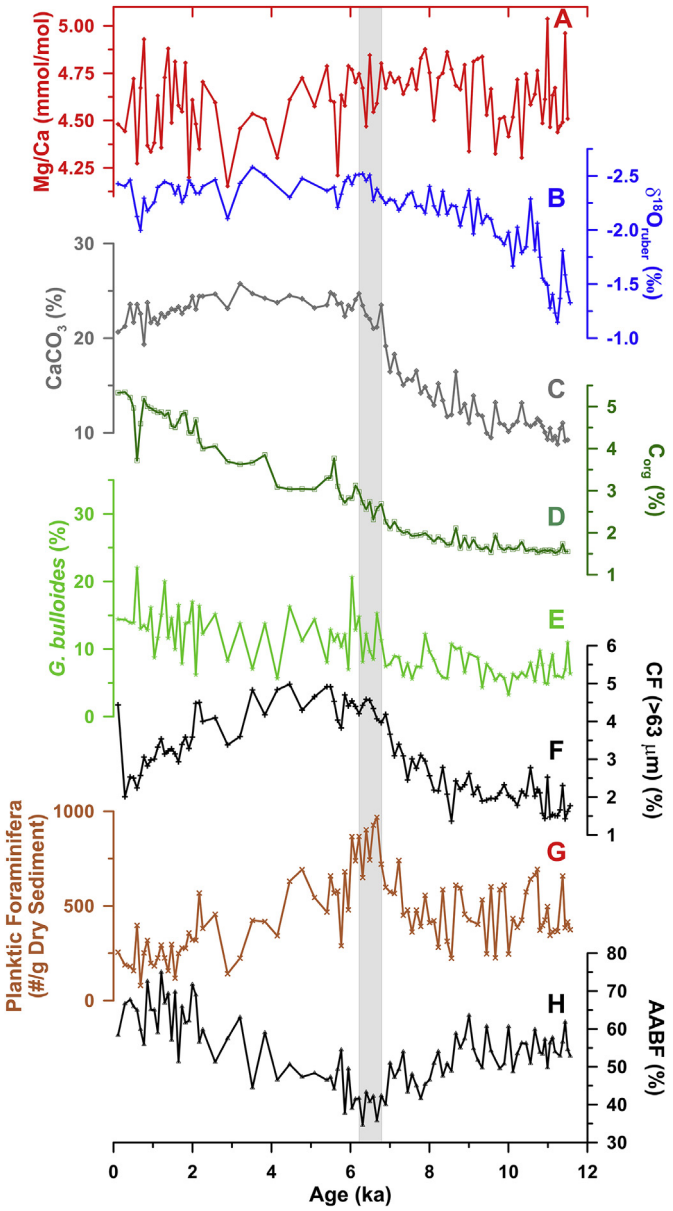

Fig. 3. Changes in faunal and geochemical parameters in the Malabar core. A. Mg/Ca ratio in *G. ruber*, a proxy for seawater temperature; B. $\delta^{18}O_{ruber}$ which has been used to determine $\delta^{18}O_{sw\text{-}ivc}$, a proxy for local precipitation-evaporation changes at the core site; C. $CaCO_3$ weight percentage; D. Organic carbon weight percentage (C_{org}); E. Relative abundance of planktic foraminifer *G. bulloides*, a proxy for primary productivity; F. Percentage of coarse fraction (CF) (>63 μm); G. Abundance of all planktic foraminifera per gram dry sediment; and H. Relative abundance of angular asymmetrical benthic foraminifera (AABF), an indicator of bottom water oxygenation. The grey bar marks the mid-Holocene transition in various proxy indicators.

https://doi.org/10.1016/j.yqres.2016.06.001 Published online by Cambridge University Press

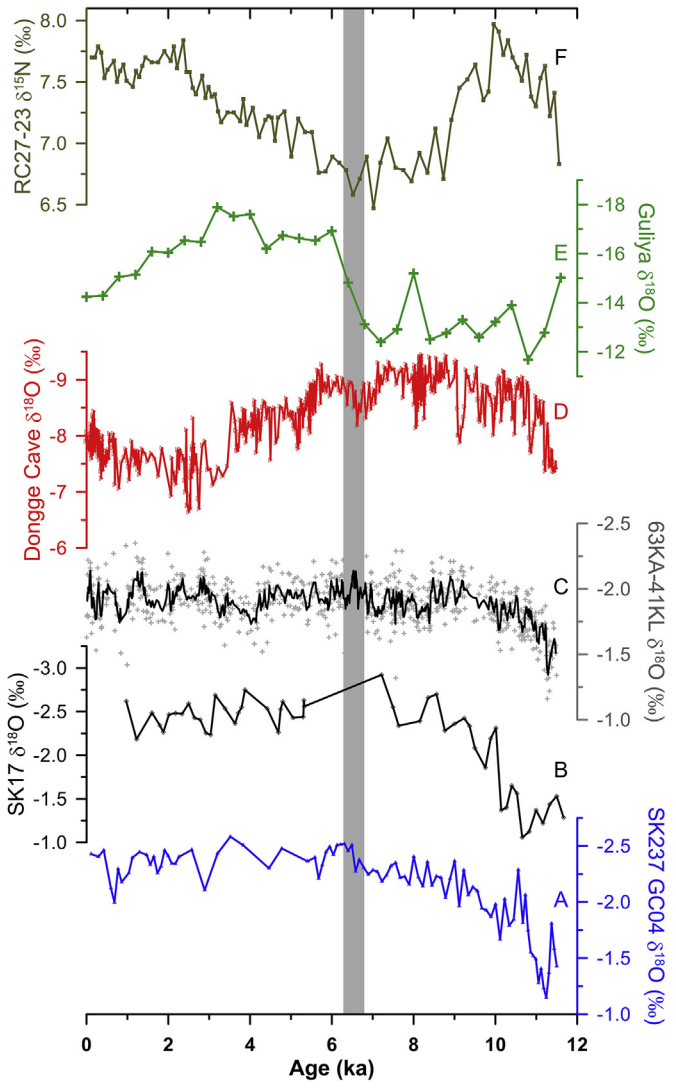

Fig. 4. Comparison of Malabar core data (A) with representative marine and terrestrial records from the Arabian Sea and Asian subcontinent (B), namely SK17 $\delta^{18}O_{ruber}$ (Anand et al., 2008), (C) 63KA-41KL $\delta^{18}O_{ruber}$ (Staubwasser et al., 2003a,b), (D) Dongge Cave speleothem $\delta^{18}O$ (Dykoski et al., 2005), (E) Guliya ice core $\delta^{18}O$ (Thompson et al., 2012) and (F) RC27-23 $\delta^{15}N$ (Altabet et al., 2002). The vertical grey bar marks the mid-Holocene transition in various proxy indicators in both the Malabar core and terrestrial records.

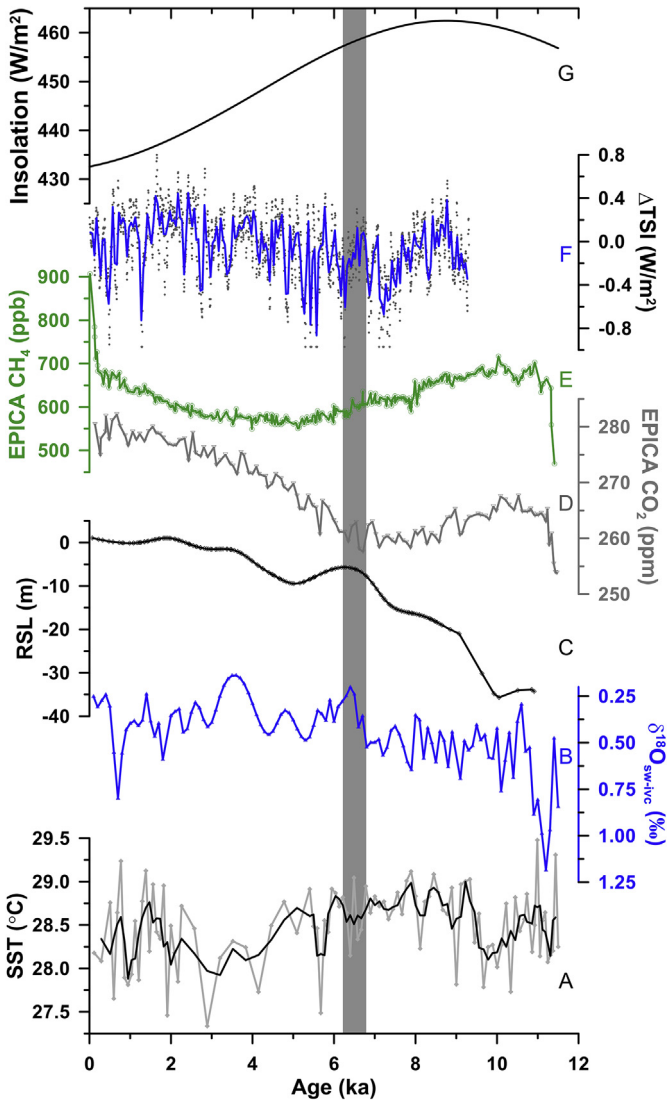

Fig. 5. A comparison of Malabar core Mg/Ca SST (the black line is 3 point running average) (A), and $\delta^{18}O_{sw\text{-}ivc}$ (B), with relative sea level (RSL) (1-ka moving Gaussian filter) (Grant et al., 2012) (C), atmospheric CO_2 (Monnin et al., 2001) (D), CH_4 from European Project for Ice Coring in Antarctica (EPICA) (Loulerge et al., 2008) (E), change in total solar irradiance (ΔTSI) (the blue line is 5 point running average) (Steinhilber et al., 2009) (F) and low-latitude insolation (Laskar et al., 2004) (G) during the Holocene. The vertical grey bar marks the mid-Holocene transition in various proxy indicators in both the Malabar core and other records.

decrease in $\delta^{18}O_{sw\text{-}ivc}$ begins at 4.4 ka and continues until 3.6 ka. The $\%CaCO_3$ increases throughout the early Holocene untill 6.2 ka, with no further increase during the late Holocene. The lowest $\%CaCO_3$ (8.8%) concentration is reported at 11.3 ka and the highest (25.8%) is at 3.2 ka. A clear increase in relative abundance of *G. bulloides* is evident during this same interval. The minimum *G. bulloides* relative abundance (3.3%) occurred during the early Holocene at 10.0 ka, while the maximum abundance (22.0%) occurred during the late Holocene at 0.6 ka. A net increase in $\%C_{org}$ is evident during the early Holocene, followed with nearly uniform values between 6.1 and 4.1 ka. The $\%C_{org}$ varied from 1.5 to 5.3% at 11.2 and 0.29 ka, respectively. The coarse fraction varied from 1.4% to 5.0% at 8.6 and 4.5 ka, respectively. The continuous gradual increase in coarse fraction during the early Holocene stopped at 6.5 ka. The relative abundance of AABF gradually decreased during the early Holocene until 6.3 ka. A gradual increase in AABF is evident during the late Holocene (Fig. 3).

Discussion

The residual $\delta^{18}O_{sw\text{-}ivc}$, obtained by subtracting global ice volume contribution from temperature corrected $\delta^{18}O$, is a proxy for seawater salinity (Weldeab et al., 2005; Govil and Naidu, 2010; Saraswat et al., 2012; Kessarkar et al., 2013). The salinity at the core site is a function of evaporation-precipitation budget. Additionally, the transport of water from the Bay of Bengal to the southeastern Arabian Sea also affects the salinity in this region (Prasanna Kumar et al., 2004). Therefore, the most enriched $\delta^{18}O_{sw\text{-}ivc}$ during the marine isotopic stage 2/1 transition, suggests an extremely weak monsoon at this time. The reduced transport of low salinity water from the Bay of Bengal during early Holocene, as inferred from relatively low Ba/Ca ratio in surface dwelling planktic foraminifera (Saraswat et al., 2013), further enriched the $\delta^{18}O_{sw\text{-}ivc}$ in the southeastern Arabian Sea (Fig. 5). The depleting $\delta^{18}O_{sw\text{-}ivc}$

https://doi.org/10.1016/j.yqres.2016.06.001 Published online by Cambridge University Press

beginning at 11.2 ka and continuing until 6.4 ka suggests a progressive strengthening of the monsoon. The short initial abrupt phase of this long gradually strengthening early Holocene monsoon change was driven by vigorous transport of low salinity water from the Bay of Bengal, as is evident from a marked increase in Ba/Ca ratio (Saraswat et al., 2013). The temperature during the short abrupt phase of early Holocene monsoon strengthening was relatively warm and stable. A prominent strengthening of monsoon is also evident between 6.8 and 6.4 ka, when the $\delta^{18}O_{sw\text{-}ivc}$ decreased by ~0.3‰, followed by an equally weakened monsoon until 5.3 ka (Fig. 5). The SST was relatively stable between 9.3 and 6.0 ka during the early Holocene phase of monsoon strengthening. An early Holocene weak monsoon phase has also been reported from Rajasthan in western India (Singh et al., 1974). The subsequent strengthening of southwest monsoon at 9.6 and 8.6 ka is attributed to changing solar radiation (Sirocko et al., 1993). In archaeological records this time coincides with the emergence of Neolithic tools during the early Holocene. The Neolithic phase is characterized by planned habitation termed early village settlement (Bellwood, 1996). Another important aspect of this phase of human development was planned food production, domestication of animals and, at later stages, introduction of pottery, which was probably supported by the onset of a stable monsoon phase (Bellwood, 1996).

A distinct change in both the geochemical and faunal proxies is observed during the mid-Holocene in the Malabar core, suggesting a climatic event that affected the southeastern Arabian Sea. The progressive strengthening of monsoon since the early Holocene, as inferred from depleting $\delta^{18}O_{sw\text{-}ivc}$, continued until 6.4 ka, followed by an increase in $\delta^{18}O_{sw\text{-}ivc}$ until 5.3 ka. The enriched $\delta^{18}O_{sw\text{-}ivc}$, post mid-Holocene transition, suggests either reduced monsoon influence and/or reduced input of low salinity water from the Bay of Bengal. The transition in $\delta^{18}O_{sw\text{-}ivc}$ is synchronous with a shift in surface productivity, decrease in both the planktic foraminiferal abundance as well as coarse-fraction abundance, suggesting a decrease in planktic foraminiferal population. The decreased surface productivity combined with the decrease in planktic foraminiferal population supports reduced monsoon influence after the mid-Holocene transition. The changes in $\%CaCO_3$ and $\%C_{org}$ are also synchronous suggesting a concomitant response of carbon burial to changes in evaporation-precipitation and productivity. The gradual increase in dissolved oxygen concentration at the sediment–water interface, until 6.3 ka, inferred from the decrease in relative abundance of angular asymmetrical benthic foraminifera, also stopped and it began to decrease after the mid-Holocene (Fig. 3). The increase in relative abundance of AABF, post mid-Holocene, suggests decrease in dissolved oxygen at the sediment–water interface.

The mid-Holocene changes in the Malabar core proxy data are also evident in stable oxygen isotopic record in other cores published from the Arabian Sea (Staubwasser et al., 2003a,b; Anand et al., 2008). A synchronous change in $\delta^{18}O_{ruber}$ is observed in core SK17 collected from the central-eastern Arabian Sea, from a comparable water depth (Anand et al., 2008). Similarly, a distinct shift towards depleted $\delta^{18}O_{ruber}$ is also evident in core 63KA-41KL (Staubwasser et al., 2003a,b). Interestingly, a distinct shift in denitrification, as inferred from changes in $\delta^{15}N$, is also evident at the same time in core RC27-23 collected from the western Arabian Sea and is synchronous with the changes in relative abundance of AABF in the Malabar core (Altabet et al., 2002, Fig. 4). A distinct change in productivity at the same time was also inferred from Ocean Drilling Program (ODP) Hole 723A, Leg 117, off Oman in the northwestern Arabian Sea (Gupta et al., 2005). Several episodes of change in productivity during the Holocene were inferred at this site, as it lies at the core of summer monsoon induced upwelling. A comparison of the Malabar core data with other cores from the southeastern Arabian Sea, as well as the Bay of Bengal, further suggests a similar change in both the $\%CaCO_3$, and $\%C_{org}$ in many of these cores, even though the magnitude and timing is different (Naidu and Malmgren, 1995; Agnihotri et al., 2003; Chauhan, 2003; Anil Kumar et al., 2005; Narayana et al., 2009; Singh et al., 2011; Ahmad et al., 2012; Naik et al., 2014). The difference in magnitude and timing of changes in the proxies, in various marine cores, is attributed to the difference in regional oceanographic features, mainly productivity, surface current direction, terrigenous input and dissolved oxygen, that affects both the flux of autochthonous and allochthonous material, and its deposition and diagenetic alteration. A few of the cores were collected from the oxygen-minimum zone, which affects the carbonate preservation, and the others are from the regions outside the oxygen-minimum zone (Canfield and Raiswell, 1991; Levin, 2003). A part of the difference in timing of transition in the cores from different parts of the Arabian Sea, is also attributed to the coarse sample resolution (usually multi-centennial to a few millennium) in most of the cores (Naidu and Malmgren, 1995; Agnihotri et al., 2003; Chauhan, 2003; Anil Kumar et al., 2005; Narayana et al., 2009; Singh et al., 2011; Ahmad et al., 2012; Naik et al., 2014), which obscures a clear comparison. In spite of the differences in physico-chemical environment prevailing at the coring sites, the commonality of the mid-Holocene transition in cores collected from the southeastern Arabian Sea, suggests that it is a regional feature.

A major shift towards highly deleted $\delta^{18}O$ is also evident during the mid-Holocene, in Guliya ice-core record (Thompson et al., 2012). A similar abrupt change to relatively drier condition, beginning at ~6.1–5.4 ka, thus coinciding exactly with the mid-Holocene transition in the Malabar core, has been inferred from C/N and $\delta^{13}C$ analysis of a core collected from Nal Sarovar, a lake in the western India (Prasad et al., 1997). Similarly, a substantial decrease in summer rainfall, between 6.5 and 4.5 ka, is also evident from the pollen and grain-size analysis of a sediment core collected from the Lunkaransar saltwater lake (Swain et al., 1983; Enzel et al., 1999). A much larger change in summer monsoon rainfall in this core was, however, evident at a later age. The mid-Holocene transition also coincides with an abrupt increase in number of artifacts recovered from the Indus valley region as well as the simulated population size (Lemmen and Khan, 2012). Therefore, a distinct change during the mid-Holocene is apparent in both the marine as well as terrestrial records, suggesting a widespread climate transition during the mid-Holocene in the Indian subcontinent and adjoining seas.

A prominent climatic transition at 4.2 ka has earlier been reported in a core collected from the shallow marine region off Pakistan, which is affected by Indus influx (Staubwasser et al., 2003a,b). This 4.2 ka event was suggested to be responsible for the major shift in the Harappan settlements in western India. In the Malabar core, a substantial cooling from 28.8 °C to 27.7 °C is evident from 4.8 to 4.2 ka as well as depleted $\delta^{18}O_{sw\text{-}ivc}$ from 0.46‰ to 0.14‰ at 4.4 to 3.6 ka, suggesting a widespread transition. The depleted $\delta^{18}O_{sw\text{-}ivc}$ across the 4.2 ka event suggests intensification of monsoon. However, the previous studies suggest drier conditions after 4.2 ka (Staubwasser et al., 2003b). Similar dry conditions after 4 ka, following a phase of intense monsoon between 10 and 4 ka, are apparent in the Badain Jaran Desert in western Inner Mongolia region of northern China (Yang et al., 2011, 2013). The increased transport of low salinity water from the Bay of Bengal is an alternate source for the depleted $\delta^{18}O_{sw\text{-}ivc}$ after 4.2 ka. As cooling accompanied the 4.2 ka event, it is highly likely that the winter monsoon current was stronger, increasing the transport of low salinity water into the southeastern Arabian Sea. The lack of Ba/Ca data in the upper part of the core does not allow us to examine the relative contribution of winter monsoon current. Mixed

https://doi.org/10.1016/j.yqres.2016.06.001 Published online by Cambridge University Press

signatures of this 4.2 ka event have also been reported from other terrestrial and marine records (MacDonald, 2011). A short-lived inundation was reported at 4.2 ka in the Lunkransar Lake (Enzel et al., 1999). The Nal Sarovar lake level dropped at 4.2 ka, as inferred from a brief increase in C/N ratio to values characteristics of terrestrial vegetation (Prasad and Enzel, 2006). One, out of the several episodes of repeated decrease in relative abundance of *G. bulloides* throughout the Holocene, in a core collected off Oman margin, that were inferred as an evidence for reduced upwelling and thus weaker monsoon winds, occurred at 4.2 ka (Gupta et al., 2003). A re-examination of the chronology of various phases of Harappan civilization suggests, however, that the 4.2 ka event does not lead to any immediate major change. The mature phase of the Indus Civilization began at 4.5 ka and continued until 3.9 ka (2500–1900 BC; Possehl, 1997).

Comparison with global records

A synchronous MHCT, is also noted in the African climate, as inferred from the multi-proxy analysis of Hole 658C drilled off Cap Blanc, Mauritania (deMenocal et al., 2000). A prominent shift from cooler to warmer temperature is observed between ~6 and ~5 ka, thus matching with the mid-Holocene transition noted in the Malabar core. A distinct change in precipitation is evident in the Mediterranean region beginning at ~6 ka (Roberts et al., 2011). Widening of tropical dry Saharan belt that abruptly terminated the Mediterranean cyclogenesis and African Humid period was also dated between 5.5 and 4.5 ka (Vincenzo and Massimo, 2015). An abrupt temperature fluctuation accompanied by increase in local salinity between 6.5 and 5.7 ka, suggesting a weaker monsoon, has also been reported from the eastern Atlantic (Weldeab et al., 2005). An abrupt change in *G. bulloides* relative abundance that matches very well with the mid-Holocene transition in Malabar core, is inferred as a shift in winds associated with summer monsoon (Gupta et al., 2005). A gradual decline in sedimentary $\delta^{15}N$ was reported between 7 and 3 ka from the oligotrophic equatorial Pacific (Kienast et al., 2008). The MHCT reported in the Arabian Sea is later than the global early to mid-Holocene climatic transition (dated between 8.2 and 7.8 ka) reported from both the equator and poles (Stager and Mayewski, 1997). A concomitant change in both the eastern and western Arabian Sea as well as the eastern Atlantic, suggests that a common mechanism controlled climatic conditions in the tropical regions. We suggest that this mid-Holocene climate shift primed the conditions for the rise and subsequent proliferation of several advance civilizations throughout the world during the late Holocene, including the Harappan Civilization (Madella and Fuller, 2006). Therefore, the mid-Holocene climate shift was an important event, which may have had a profound influence on the development of human settlements during the Holocene.

Causes and consequences

The MHCT, as evident in the eastern Arabian Sea, can be brought by a change in the tropical processes, including the monsoon. The monsoon is basically driven by latitudinal position of inter-tropical-convergence-zone (ITCZ) combined with the land-ocean pressure gradient at present as well as in the past (Haug et al., 2001; Gadgil, 2003; Fleitmann et al., 2007). Both the latitudinal position and seasonal shifts in ITCZ, as well as the land ocean pressure gradient, primarily depend on temperature. As the insolation influences global temperature, the Malabar core data was compared with long-term trends in the low latitude July insolation (Laskar et al., 2004). Although the mid-Holocene transition evident in marine and terrestrial records from eastern Arabian Sea and Indian subcontinent, coincides with the decreasing phase of low-latitude insolation, the decrease in July insolation began much earlier at ~8 ka than the transition in the Malabar core (Fig. 5). In addition to the long-term orbital configuration induced insolation changes, solar activity causes short-term frequent variation in the total solar irradiance (TSI). Changes in TSI (ΔTSI) have widespread impact on Earth's climate, including the Asian monsoon (Gupta et al., 2005; Nigam et al., 1995; Wang et al., 2005). A comparison of the Malabar core record with the Holocene TSI records (Steinhilber et al., 2009) reveals that the mid-Holocene climatic transition coincides with large variation in ΔTSI (Steinhilber et al., 2009, Fig. 5). However, several large-scale fluctuations are also noted in ΔTSI, prior to and after the mid-Holocene transition. Atmospheric CO_2 concentration is also tightly coupled with global climate, especially temperature (Marcott et al., 2014). A prominent shift in atmospheric CO_2 concentration towards a continuously increasing trend is evident during the mid-Holocene. Therefore, we suggest that the combined effect of continuously decreasing summer insolation and other associated processes in combination with perturbations in TSI drove the MHCT.

As the Malabar core is located in the slope region, temporal changes in the oceanographic processes near the core site should also be seen in the context of long-term regional sea-level changes. The continental shelf gets exposed during the glacial drop in sea level and the subsequent interglacial rise in sea level, inundates the shelf. The exposure and inundation of the continental shelf during glacial-interglacial transitions, affects the surface circulation as well as the material flux pathways and its spatial extent. At present, a majority of the terrestrial runoff is restricted to the inner shelf (Chauhan et al., 2011, 2012) and during the times of low sea-stand, the same material will reach deeper regions, thus affecting the flux and subsequent digenetic processes. The entire continental shelf was exposed during the last glacial maximum, as a result of lowering of sea level by ~120 m (Siddall et al., 2003; Grant et al., 2012). The subsequent inundation of the shelf, affected the spatial extent of terrigenous input as well as the coastal current intensity and direction in the southeastern Arabian Sea (Ramaswamy and Nair, 1989; Chauhan et al., 2000, 2011). A comparison of the core data with the regional as well as global sea-level curve, reveals a relative stabilization of the sea level only at ~6.4 ka (Hashimi et al., 1995; Siddall et al., 2003; Grant et al., 2012), suggesting that the sea level changes also contributed towards the mid-Holocene transition noted in the Malabar and other cores (Staubwasser et al., 2003a,b; Anand et al., 2008; Naik et al., 2014) collected from the southeastern Arabian Sea.

The mid-Holocene change in local evaporation-precipitation is synchronous with the surface productivity, carbonate burial and bottom water dissolved oxygen, within age uncertainties. As perturbations in tropical rainfall are reflected in global methane records, the Malabar core data was compared with ice-core methane records for the Holocene. The signatures of this monsoon driven mid-Holocene transition are, however, not reflected in the ice-core methane records until ~5 ka (Loulerge et al., 2008, Fig. 5). Therefore, the mid-Holocene transition as recorded in the Malabar and other cores collected from the southeastern Arabian Sea, as well as in the terrestrial regions, was not strong enough to tweak the global methane concentration until ~5 ka. A synchronous change is, however, seen in atmospheric carbon-dioxide concentration as it continuously increases after ~6.5 ka (Monnin et al., 2001). The widespread nature of MHCT in Indian as well as other global records is intriguing. The possible reason for the widespread nature of MHCT is that at present as well as in the past, the monsoon in this region is driven by latitudinal position of inter-tropical-convergence-zone (ITCZ) (Haug et al., 2001; Gadgil, 2003; Fleitmann et al., 2007). We argue that ITCZ is the key driver

https://doi.org/10.1016/j.yqres.2016.06.001 Published online by Cambridge University Press

responsible for the synchronous transition in not only African and Indian climate but also other global climate systems.

We suggest that this mid-Holocene climate shift primed the conditions for the rise and subsequent proliferation of several advanced civilizations of the world. The broad time bracket for the mature phase of the Indus Civilization is regarded to be 4.5 to 3.9 ka (2500–1900 BC; Possehl, 1997). Agrawal and Kusumgar (1974) proposed a time bracket for mature Harappan phase at 4.3 to 4.0 ka (2300–2000 BC) for nuclear region and 4.2 to 3.7 ka (2200–1700 BC) for peripheral zone of Harappan Civilization. Later, Allchin and Allchin (1988) also proposed the same chronology for the mature phase of the Indus civilization. Subsequently, many chalcolithic cultures flourished in several parts of southeastern Rajasthan, western MP, and Maharashtra during 4.0 to 3.0 ka (2000–1000 BC) (Sankalia, 1968). The trade connection between Indus and Mesopotamian civilization also flourished during 2300 to 1900 BC (Gadd and Smith, 1924).

Conclusions

Centennial scale change in seawater temperature, evaporation-precipitation, carbonate burial and upwelling induced productivity were reconstructed from the southeastern Arabian Sea using faunal and geochemical proxies. We report a major shift in proxies during the mid-Holocene from 6.8 to 6.2 ka. A comparison of the Malabar core data with previously published records shows the regional nature of the MHCT. The MHCT is also evident in the terrestrial records. The widespread nature of the MHCT event in both the marine and terrestrial records suggests that the mid-Holocene transition recorded in the Malabar core, affected the entire Asia and adjoining seas. A similar shift in the African climate, during the mid-Holocene, suggests that a common mechanism was responsible for the mid-Holocene transition in the tropical regions. We propose that this MHCT primed the conditions for the rise and subsequent proliferation of several advanced civilizations of the world.

Acknowledgments

The authors are thankful to Georges Paradis for the elemental analysis, Prof. Andreas Mackensen and the staff at the stable isotopic laboratory of the Alfred Wegner Institute for Polar and Marine Research, Bremerhaven for the stable oxygen isotopic analysis and Dr. Prakash Babu, for the help in inorganic and organic carbon analysis. Authors are thankful to Editor Professor Lewis Owen, Associate Editor Professor Ashok Singhvi, and two anonymous reviewers for their constructive comments and suggestions, which helped us improve an early version of our manuscript. RS is thankful to the Department of Science and Technology, India for granting the FASTRACK project (Grant No. SR/FTP/ES-68/2009) and Indo-US Science and Technology Forum for the fellowship (Grant No. IUSSTF Fellowships/2009/1-Rajeev Saraswat) to visit University of California, Santa Barbara, USA. Authors thankfully acknowledge the financial support from the Council of Scientific and Industrial Research, India to the GEOSINKS project.

References

Acker, J.G., Leptoukh, G., 2007. Online analysis enhances use of NASA Earth science data. Eos Transaction AGU 88 14.
Agnihotri, R., Bhattacharya, S.K., Sarin, M.M., Somayajulu, B.L.K., 2003. Changes in surface productivity and subsurface denitrification during the Holocene: a multiproxy study from the eastern Arabian Sea. Holocene 13, 701–713.
Agrawal, D.P., Kusumgar, 1974. Prehistoric Chronology and Radiocarbon Dating in India (New Delhi).
Ahmad, S.M., Zheng, H., Raza, W., Zhou, B., Lone, M.A., Raza, T., Suseela, G., 2012. Glacial to Holocene changes in the surface and deep waters of the northeast Indian Ocean. Marine Geology 329–331, 16–23.
Allchin, B., Allchin, R., 1988. The Rise of Civilization in India and Pakistan. Cambridge University Press, Cambridge.
Altabet, M.A., Higginson, M.J., Murray, D.W., 2002. The effect of millennial-scale changes in Arabian Sea denitrification on atmospheric CO_2. Nature 415, 159–162.
Anand, P., Kroon, D., Singh, A.D., Ganeshram, R.S., Ganssen, G., Elderfield, H., 2008. Coupled sea surface temperature–seawater $\delta^{18}O$ reconstructions in the Arabian Sea at the millennial scale for the last 35 ka. Paleoceanography 23, PA4207. http://dx.doi.org/10.1029/2007PA001564.
Anil Kumar, A., Rao, V.P., Patil, S.K., Kessarkar, P.M., Thamban, M., 2005. Rock magnetic records of the sediments of the eastern Arabian Sea: evidence for late Quaternary climatic change. Marine Geology 220, 59–82.
Bellwood, P., 1996. The origins and spread of agriculture in the Indo-Pacific region: gradualism and diffusion or revaluations and colonization? In: Haris, D.R. (Ed.), The Origins and Spread of Agriculture and Pastoralism in Eurasia. UCL Press, London, pp. 465–498.
Canfield, D.E., Raiswell, R., 1991. Carbonate precipitation and dissolution. In: Allison, P.A., Briggs, D.E.G. (Eds.), Taphonomy: Releasing the Data Locked in the Fossil Record. Plenum Press, New York, pp. 411–453.
Chauhan, O.S., 2003. Past 20,000-year history of Himalayan aridity: evidence from oxygen isotope records in the Bay of Bengal. Current Science 84, 90–93.
Chauhan, O.S., Almeida, F., Suneethi, J., 2000. Influence of sedimentation on the geomorphology of the northwestern continental margin of India. Marine Geodesy 23, 259–265.
Chauhan, O.S., Raghavan, B.R., Singh, K., Rajawat, A.S., Ajai, Kader, U.S.A., Nayak, S., 2011. Influence of orographically enhanced SW monsoon flux on coastal processes along the SE Arabian Sea. Journal of Geophysical Research 116, C12037. http://dx.doi.org/10.1029/2011JC007454.
Cook, B.I., Ault, T.R., Smerdon, J.E., 2015. Unprecedented 21st century drought risk in the American southwest and central plains. Science Advances 1, e1400082.
deMenocal, P., Ortiz, J., Guilderson, T., Sarnthein, M., 2000. Coherent high- and low-latitude climate variability during the Holocene warm period. Science 288, 2198–2202.
Dixit, Y., Hodell, D.A., Petrie, C.A., 2014. Abrupt weakening of the summer monsoon in northwest India ~4100 yr ago. Geology 42, 339–342. http://dx.doi.org/10.1130/G35236.1.
Dykoski, C.A., Edwards, R.L., Cheng, H., Yuan, D., Cai, Y., Zhang, M., Lin, Y., Qing, J., An, Z., Revenaugh, J., 2005. A high-resolution, absolute dated Holocene and deglacial Asian monsoon record from Dongge Cave, China. Earth and Planetary Science Letters 233, 71–86.
Enzel, Y., Ely, L.L., Mishra, S., Ramesh, R., Amit, R., Lazar, B., Rajaguru, S.N., Baker, V.R., Sandler, A., 1999. High resolution Holocene environmental changes in the Thar Desert, northwestern India. Science 284, 125–128.
Fleitmann, D., Burns, S.J., Mangini, A., Mudelsee, M., Kramers, J., Villa, I., Neff, U., Al-Subbary, A.A., Buettner, A., Hippler, D., Matter, A., 2007. Holocene ITCZ and Indian monsoon dynamics recorded in stalagmites from Oman and Yemen (Socotra). Quaternary Science Reviews 26, 170–188.
Gadd, C.J., Smith, S., 1924. The New Links between India and Babylonian Civilizations. Illustrated London News, 4 October, pp. 614–616.
Gadgil, S., 2003. The Indian monsoon and its variability. Annual Review of Earth Planetary Sciences 31, 429–467.
Govil, P., Naidu, P.D., 2010. Evaporation-precipitation changes in the eastern Arabian Sea for the last 68 ka: implications on monsoon variability. Paleoceanography 25, PA1210. http://dx.doi.org/10.1029/2008PA001687.
Grant, K.M., Rohling, E.J., Bar-Matthews, M., Ayalon, A., Medina-Elizalde, M., Bronk Ramsey, C., Satow, C., Roberts, A.P., 2012. Rapid coupling between ice volume and polar temperature over the past 150 kyr. Nature 491, 744–747.
Gupta, A.K., Anderson, D.M., Overpeck, J.T., 2003. Abrupt changes in the Asian southwest monsoon during the Holocene and their links to the North Atlantic Ocean. Nature 421, 354–357.
Gupta, A.K., Das, M., Anderson, D.M., 2005. Solar influence on the Indian summer monsoon during the Holocene. Geophysical Research Letters 32, L17703. http://dx.doi.org/10.1029/2005GL022685.
Hashimi, N.H., Nigam, R., Nair, R.R., Rajagopalan, G., 1995. Holocene sea level fluctuations on western Indian continental margin: an update. Journal Geological Society of India 46, 157–162.
Haug, G.H., Hughen, K.A., Sigman, D.M., Peterson, L.C., Rohl, U., 2001. Southward migration of the intertropical convergence zone through the Holocene. Science 293, 1304–1308.
Kelly, R.L., Surovell, T.A., Shuman, B.N., Smith, G.M., 2013. A continuous climatic impact on Holocene human population in the Rocky Mountains. Proceedings National Academy of Sciences 110, 443–447.
Kessarkar, P.M., Rao, V.P., Naqvi, S.W.A., Karapurkar, S.G., 2013. Variation in the Indian summer monsoon intensity during the Bølling-Allerød and Holocene. Paleoceanography 28. http://dx.doi.org/10.1002/palo.20040.
Kienast, M., Lehmann, M.F., Timmermann, A., Galbraith, E., Bolliet, T., Holbourn, A., Normandeau, C., Laj, C., 2008. A mid-Holocene transition in the nitrogen dynamics of the western equatorial Pacific: evidence of a deepening thermocline? Geophysical Research Letters 35, L23610.
Laskar, J., Robutel, P., Joutel, F., Gastineau, M., Correia, A.C.M., Levrard, B., 2004. A long term numerical solution for the insolation quantities of the Earth. Astronomy and Astrophysics 428, 261–285.

Lea, D.W., Mashiotta, T.A., Spero, H.J., 1999. Controls on magnesium and strontium uptake in planktonic foraminifera determined by live culturing. Geochemica Cosmochemica Acta 63, 2369–2379.
Lemmen, C., Khan, A., 2012. A simulation of the neolithic transition in the Indus Valley. In: Giosan, L., Fuller, D.Q., Nicoll, K., Flad, R.K., Clift, P.D. (Eds.), Climates, Landscapes, and Civilizations, Geophys. Monogr. Ser, 198. AGU, Washington, D. C., pp. 107–114. http://dx.doi.org/10.1029/GM198
Levin, L.A., 2003. Oxygen minimum zone benthos: adaptation and community response to hypoxia. Oceanography and Marine Biology: an Annual Review 41, 1–45.
Lévy, M., Shankar, D., André, J.-M., Shenoi, S.S.C., Durand, F., de Boyer Montégut, C., 2007. Basin-wide seasonal evolution of the Indian Ocean's phytoplankton blooms. J. Geophys. Res. 112 (C12014) http://dx.doi.org/10.1029/2007JC004090.
Loulerge, L., Schilt, A., Spahni, R., Masson-Delmotte, V., Blunier, T., Lemieux, B., Barnola, J.-M., Raynaud, D., Stocker, T.F., Chappellaz, J., 2008. Orbital and millennial-scale features of atmospheric CH_4 over the past 800,000 years. Nature 453, 383–386.
MacDonald, G., 2011. Potential influence of the Pacific Ocean on the Indian summer monsoon and Harappan decline. Quaternary International 229, 140–148.
Madella, M., Fuller, D.Q., 2006. Palaeoecology and the Harappan civilisation of South Asia: a reconsideration. Quaternary Science Reviews 25, 1283–1301.
Marcott, S.A., Bauska, T.K., Buizert, C., Steig, E.J., Rosen, J.L., Cuffey, K.M., Fudge, T.J., Severinghaus, J.P., Ahn, J., Kalk, M.L., McConnell, J.R., Sowers, T., Taylor, K.C., White, J.W.C., Brook, E.J., 2014. Centennial-scale changes in the global carbon cycle during the last deglaciation. Nature 514, 616–619.
Monnin, E., Indermuhle, A., Dallenbach, A., Flückiger, J., Stauffer, B., Stocker, T.F., Raynaud, D., Barnola, J.-M., 2001. Atmospheric CO_2 concentrations over the last glacial termination. Science 291, 112–114.
Naidu, P.D., Malmgren, B.A., 1995. A 2200 years periodicity in the Asian monsoon system. Geophysical Research Letters 22, 2361–2364.
Naik, S.S., Godad, S.P., Naidu, P.D., Tiwari, M., Paropkari, A.L., 2014. Early- to late-Holocene contrast in productivity, OMZ intensity and calcite dissolution in the eastern Arabian Sea. The Holocene 24, 749–755.
Narayana, A.C., Naidu, P.D., Shinu, N., Nagabhushanam, P., Sukhija, B.S., 2009. Carbonate and organic carbon content changes over last 20 ka in the southeastern Arabian Sea: Paleoceanographic implications. Quaternary International 206, 72–77.
Naqvi, S.W.A., 1991. Geographical extent of denitrification in the Arabian Sea in relation to some physical processes. Oceanologica Acta 14, 281–290.
Naqvi, S.W.A., Jayakumar, D.A., Narvekar, P.V., Naik, H., Sarma, V.V.S.S., DeSouza, W., Joseph, S., George, M.D., 2000. Increased marine production of N_2O due to intensifying anoxia on the Indian continental shelf. Nature 408, 346–349.
Naqvi, S.W.A., Naik, H., Narvekar, P.V., 2003. The Arabian Sea. In: Black, K., Shimmield, G.B. (Eds.), Biogeochemistry of Marine Systems. Oxford, UK, pp. 157–207.
Nigam, R., Khare, N., Borole, D.V., 1992. Can benthic foraminiferal morpho-groups be used as indicators of paleomonsoonal precipitation? Estuarine Coastal and Shelf Science 34, 533–542.
Nigam, R., Khare, N., Nair, R.R., 1995. Foraminiferal evidences for 77-year cycles of droughts in India and its possible modulation by the Gleissberg solar cycle. Journal of Coastal Research 11, 1099–1107.
Nigam, R., Mazumder, A., Henriques, P.J., Saraswat, R., 2007. Benthic foraminifera as proxy for oxygen-depleted conditions off the central west coast of India. Journal Geological Society of India 70, 1047–1054.
Possehl, G.L., 1997. The transformation of the Indus civilization. Journal of World Prehistory 11, 425–472.
Prasad, S., Enzel, Y., 2006. Holocene paleoclimates of India. Quaternary Research 66, 442–453.
Prasad, S., Kusumgar, S., Gupta, S.K., 1997. A mid–late Holocene record of palaeoclimatic changes from Nal Sarovar-A palaeodesert margin lake in western India. Journal of Quaternary Science 12, 153–159.
Prasanna Kumar, S., Narvekar, J., Kumar, A., Shaji, C., Anand, P., Sabu, P., Rejomon, G., Jacob, J., Jayaraj, K.A., Radhika, A., Nair, K.K.C., 2004. Intrusion of the Bay of Bengal water into the Arabian Sea during winter monsoon and associated chemical and biological response. Geophysical Research Letters 31 (L15304).
Ramaswamy, V., Nair, R.R., 1989. Lack of cross-shelf transport of sediments on the western margin of India: evidence from clay mineralogy. Journal of Coastal Research 5, 541–545.
Reimer, P.J., Baillie, M.G.L., Bard, E., Bayliss, A., Beck, J.W., Blackwell, P.G., Ramsey, C.B., Buck, C.E., Burr, G.S., Edwards, R.L., Friedrich, M., Grootes, P.M., Guilderson, T.P., Hajdas, I., Heaton, T.J., Hogg, A.G., Hughen, K.A., Kaiser, K.F., Kromer, B., McCormac, F.G., Manning, S.W., Reimer, R.W., Richards, D.A., Southon, J.R., Talamo, S., Turney, C.S.M., van der Plicht, J., Weyhenmeyer, C.E., 2009. Intcal09 and Marine09 radiocarbon age calibration curves, 0-50,000 years cal BP. Radiocarbon 51, 1111–1150.
Roberts, N., Brayshaw, D., Kuzucuoglu, C., Perez, R., Sadori, L., 2011. The mid-Holocene climatic transition in the Mediterranean: causes and consequences. The Holocene 21, 3–13.
Ruddiman, W.F., Ellis, E.C., 2009. Effect of per-capita land use changes on Holocene forest clearance and CO_2 emissions. Quaternary Science Reviews 28, 3011–3015.
Sankalia, H.D., 1968. Prehistory and Protohistory of India and Pakistan. Bombay University, Bombay.
Saraswat, R., Nigam, R., Weldeab, S., Mackensen, A., Naidu, P.D., 2005. A first look at past sea surface temperatures in the equatorial Indian Ocean from Mg/Ca in foraminifera. Geophysical Research Letters 32, L24605. http://dx.doi.org/10.1029/2005GL024093.
Saraswat, R., Nigam, R., Mackensen, A., Weldeab, S., 2012. Linkage between seasonal insolation gradient in the tropical northern hemisphere and the sea surface salinity of the equatorial Indian Ocean during the last glacial period. Acta Geologica Sinica 86, 801–811.
Saraswat, R., Lea, D.W., Nigam, R., Mackensen, A., Naik, D.K., 2013. Deglaciation in the tropical Indian Ocean driven by interplay between the regional monsoon and global teleconnections. Earth and Planetary Science Letters 375, 166–175.
Sarkar, A., Ramesh, R., Somayajulu, B.L.K., Agnihotri, R., Jull, A.J.T., Burr, G.S., 2000. High resolution Holocene monsoon record from the eastern Arabian Sea. Earth and Planetary Science Letters 177, 209–218.
Schewe, J., Levermann, A., 2012. A statistically predictive model for future monsoon failure in India. Environmental Research Letters 7. http://dx.doi.org/10.1088/1748-9326/7/4/044023.
Shankar, D., Vinaychandran, P.N., Unnikrishnan, A.S., 2002. The monsoon currents in the north Indian Ocean. Prog. Oceanogra 52, 63–120.
Shenoi, S.S.C., Shankar, D., Shetye, S.R., 1999. The sea surface temperature high in the Lakshadweep Sea before the onset of the southwest monsoon. Journal of Geophysical Research 104, 703–712.
Siddall, M., Rohling, E.J., Almogi-Labin, A., Hemleben, Ch., Meischner, D., Schmelzer, I., Smeed, D.A., 2003. Sealevel fluctuations during the last glacial cycle. Nature 423, 853–858.
Singh, A.D., Jung, S.J.A., Darling, K., Ganeshram, R., Ivanochko, T., Kroon, D., 2011. Productivity collapses in the Arabian Sea during glacial cold phases. Paleoceanography 26, PA3210. http://dx.doi.org/10.1029/2009PA001923.
Singh, G., Joshi, R.D., Chopra, S.K., Singh, A.B., 1974. Late Quaternary history of vegetation and climate of the Rajasthan Desert, India. Philosophical Transactions of The Royal Society of London Series B 267, 467–501.
Sinha, R., Smykatz-Kloss, W., Stüben, D., Harrison, S.P., Berner, Z., Kramar, U., 2006. Late Quaternary palaeoclimatic reconstruction from the lacustrine sediments of the Sambhar playa core, Thar Desert margin, India. Palaeogeography, Palaeoclimatology, Palaeoecology 233, 252–270.
Sirocko, F., Sarnthein, M., Erlenkeuser, H., Lange, H., Arnold, A., Duplessy, J.C., 1993. Century-scale events in monsoonal climate over the past 24,000 years. Nature 364, 322–324.
Southon, J., Kashgarian, M., Fontugne, M., Metivier, B., Yim, W.W.-S., 2002. Marine reservoir corrections for the Indian Ocean and Southeast Asia. Radiocarbon 44, 167–180.
Stager, J.C., Mayewski, P.A., 1997. Abrupt early to mid-Holocene climatic transition registered at the equator and the poles. Science 276, 1834–1836.
Staubwasser, M., et al., 2003a. Arabian Sea Cores 63KA, 41KL, 42KG Foraminiferal Oxygen Isotope Data, IGBP PAGES/World Data Center for Paleoclimatology Data Contribution Series # 2003-059 (NOAA/NGDC Paleoclimatology Program, Boulder CO, USA).
Staubwasser, M., Sirocko, F., Grootes, P.M., Segl, M., 2003b. Climate change at the 4.2 ka BP termination of the Indus valley civilization and Holocene south Asian monsoon variability. Geophysical Research Letters 30, 1425. http://dx.doi.org/10.1029/2002GL016822.
Steinhilber, F., Beer, J., Fröhlich, C., 2009. Total solar irradiance during the Holocene. Geophysical Research Letters 36, L19704. http://dx.doi.org/10.1029/2009GL040142.
Stuiver, M., Reimer, P.J., 1993. Extended ^{14}C database and revised CALIB radiocarbon calibration program. Radiocarbon 35, 215–230.
Swain, A.M., Kutzbach, J.E., Hastenrath, S., 1983. Estimates of Holocene precipitation for Rajasthan, India, based on pollen and lake level data. Quaternary Research 19, 1–17.
Thompson, L.G., Yao, T., Davis, M.E., Henderson, K.A., Mosley-Thompson, E., Lin, P.-N., Beer, J., Synal, H.-A., Cole-Dai, J., Bolzan, J.F., 2012. Guliya Ice Core 128 Ka Isotope, Dust, Anion, and Accumulation Data. IGBP PAGES/World Data Center for Paleoclimatology, Data Contribution Series # 2012–011.
Vincenzo, De Santis, Massimo, C., 2015. The 5.5-4.5 ka climatic transition as recorded by the sedimentation pattern of coastal deposits of the Apulia region, southern Italy. Holocene 1–17.
Wang, Y.J., Cheng, H., Edwards, R.L., He, Y., Kong, X., An, Z., Wu, J., Kelly, M.J., Dykoski, C.A., Li, X., 2005. The Holocene Asian monsoon: links to solar changes and North Atlantic climate. Science 308, 854–857.
Weldeab, S., Schneider, R.R., Kölling, M., Wefer, G., 2005. Holocene African droughts relate to eastern equatorial Atlantic cooling. Geology 33, 981–984.
Yadav, R.R., Braeuning, A., Singh, J., 2011. Tree ring inferred summer temperature variations over the last millennium in western Himalaya, India. Climate Dynamics 36, 1545–1554.
Yang, X., Scuderi, L., Paillou, P., Liu, Z., Li, H., Ren, X., 2011. Quaternary environmental changes in the drylands of China – a critical review. Quaternary Science Reviews 30, 3219–3233.
Yang, X., Wang, X., Liu, Z., Li, H., Ren, X., Zhang, D., Ma, Z., Rioual, P., Jin, X., Scuderi, L., 2013. Initiation and variation of the dune fields in semi-arid China – with a special reference to the Hunshandake Sandy Land, Inner Mongolia. Quaternary Science Reviews 78, 369–380.

https://doi.org/10.1016/j.yqres.2016.06.001 Published online by Cambridge University Press